frontiers | Frontiers in Marine Science

TYPE Original Research
PUBLISHED 04 April 2023
DOI 10.3389/fmars.2023.1114809

OPEN ACCESS

EDITED BY
Leonie Esters,
University of Bonn, Germany

REVIEWED BY
Kaiming Hu,
Institute of Atmospheric Physics, Chinese Academy of Sciences (CAS), China
Fei Ge,
Chengdu University of Information Technology, China

*CORRESPONDENCE
Li Yan
yanli@gdou.edu.cn
Jianjun Xu
jxu@gdou.edu.cn

SPECIALTY SECTION
This article was submitted to Physical Oceanography, a section of the journal Frontiers in Marine Science

RECEIVED 02 December 2022
ACCEPTED 22 March 2023
PUBLISHED 04 April 2023

CITATION
Chen Y, Yan L, Xu J, Zheng S, Chen G and Lin P (2023) Climate impacts of 2009/2010 mixed-type El Niño on double ITCZs over the eastern Pacific Ocean.
Front. Mar. Sci. 10:1114809.
doi: 10.3389/fmars.2023.1114809

Climate impacts of 2009/2010 mixed-type El Niño on double ITCZs over the eastern Pacific Ocean

Yinlan Chen[1,2], Li Yan[1]*, Jianjun Xu[1]*, Shaojun Zheng[1], Guihua Chen[3] and Peixian Lin[2]

[1]College of Ocean and Meteorology/South China Sea Institute of Marine and Meteorology, Guangdong Ocean University, Zhanjiang, Guangdong, China, [2]Shanwei Meteorological Service, Shanwei, Guangdong, China, [3]Lufeng Meteorological Service, Shanwei, Guangdong, China

A double intertropical convergence zone (ITCZ) pattern emerges over the eastern Pacific Ocean in March-April. Their inter-annual variabilities may exert major climatic and ecological effects. El Niño-Southern Oscillation (ENSO) can significantly regulate the inter-annual variability of double ITCZs. ENSO diversity has increased in recent years. A mixed-type El Niño occurred in 2009/2010. Our results reveal that the meridional SSTA pattern in mixed-type El Niño is a combination of "SST warming with a maximum at the equator" (i.e., EP-type delta SST) and "north-warm and south-cold" (i.e., CP-type delta SST) patterns. In a mixed-type El Niño, both meridional EP-type and CP-type delta SST played a role and had corresponding climate impacts. Under the coordinated modulation of EP-type and CP-type delta SST in a mixed-type El Niño, the climate effect of EP-type delta SST (increasing equatorial precipitation) is weakened; while the climate effect of CP-type delta SST (enhancing the northern ITCZ and weakening the southern ITCZ) is amplified. The climate effect of mixed-type El Niño finally resembles that of typical CP-type El Niños, intensifying the north-south asymmetry of the eastern Pacific double ITCZs. This study will contribute to a better understanding of the impacts of ENSO diversity on double ITCZs in the eastern Pacific region.

KEYWORDS

mixed-type El Niño, double ITCZs, meridional EP-type delta SST, meridional CP-type delta SST, eastern Pacific Ocean, boreal spring

1 Introduction

The intertropical convergence zone (ITCZ) is a long-standing large weather system between the subtropical high belts in the northern and southern hemispheres. The ITCZ can be featured by deep convection (Xie and Yang, 2014) and intense rainfall (Philander et al., 1996; Zhang, 2001), and tends to situate on the warmest sea surface temperature (SST). As an important tropical climatic system, the ITCZ has remarkable local and remote

climate impacts. The location and intensity of ITCZ has a direct climatic impact over the eastern Pacific Ocean (e.g., Xie and Yang, 2014; Yan and Li, 2018). ITCZs can also influence the frequencies and tracks of summer tropical cyclones (e.g., Cao et al., 2013).

Accompanied by the convergence of the cross-equatorial southerly winds and the northeasterly winds in the northern hemisphere, a cold tongue over the equatorial eastern Pacific Ocean results in a belt of heavy precipitation in the northern hemisphere throughout the whole year. This heavy rainfall belt (northern ITCZ) has a distinctive seasonal evolution. Its position fluctuated in the north-south direction, reaching the northernmost point in September.

Particularly, during the boreal spring (March-April), a double-ITCZ pattern emerges over the eastern Pacific Ocean, with a strong northern ITCZ and a weak southern ITCZ (Zhang, 2001; Gu et al., 2005; Larkin and Harrison, 2005). Except for a perennial northern ITCZ, a weak ITCZ also appears in the southern hemisphere, accompanied by a weakened cross-equatorial southerly winds and a weakened equatorial cold tongue (Zhang, 2001; Gu et al., 2005; Larkin and Harrison, 2005; Yan and Li, 2018). Considering such double ITCZs over the eastern Pacific Ocean distinctively occur in March-April, the present study focuses on this season.

Previous studies showed that the El Niño events can remarkably modulate the inter-annual variability of the double ITCZs during the boreal spring (Lietzke et al., 2001; Zhang, 2001; Gu et al., 2005; Henke et al., 2012; Haffke et al., 2016; Xie et al., 2018; Yan and Li, 2018; Zhu et al., 2018). El Niño-Southern Oscillation (ENSO) has diversity, different types of El Niños have different climate impacts on such double ITCZs. The eastern Pacific-type (EP-type) El Niños (Rasmusson and Carpenter, 1982; Kug et al., 2009) drive the southern and northern ITCZs to move equatorward, which lead the double ITCZs change to be a broad equatorial ITCZ belt, and finally weaken the north-south asymmetry of the eastern Pacific double ITCZs. In contrast, the central Pacific-type (CP-type) El Niños (Ashok et al., 2007; Kao and Yu, 2009; Li et al., 2010; Yan and Li, 2018) further strengthen the north-south asymmetry of the double ITCZs by strengthening the northern ITCZ and weakening the southern ITCZ.

In addition to typical EP-type and CP-type El Niños, there are also mixed-type El Niños with characteristics of both EP-type and CP-type El Niños. The 2009/2010 El Niño is recognized as a nonconventional event (Zhang et al., 2013) and exhibits a unique time-space variation of the SST and subsurface structure (Kim et al., 2011). The previous study (Yu and Kim, 2013) considered a mixed-type El Niño as the simultaneous occurrence of EP-type and CP-type El Niños. In consistent with Yu and Kim (2013), according to the standard that both the EP index (Niño-3 index) and CP index (El Niño Modoki index, EMI) exceeded about 0.8 standard deviation in January-February and March-April, the 2009/2010 event was selected as a mixed-type El Niño.

The inter-annual variability of double ITCZs may exert major climatic and ecological effects. Different types of El Niños can significantly regulate double ITCZs' inter-annual variabilities. The climate impacts of typical EP-type and CP-type El Niños on double ITCZs in the decaying year of El Niños have been studied. However, the climate impacts of a mixed-type El Niño event with both EP-type and CP-type characteristics on the double ITCZs remain unclear. In this study, we found that the meridional EP-type delta SST and CP-type delta SST were comparable in this mixed-type event. Based on this, the present study focuses on the modulation features of the 2009/2010 mixed-type El Niño on double ITCZs, and contrasts its effects with those of typical EP-type and CP-type El Niños. Our results reveal that under the coordinated modulation of EP-type delta SST and CP-type delta SST, the modulation of EP-type delta SST is suppressed and the modulation of CP-type delta SST is amplified.

2 Data and methods

The data were provided by the European Center for Medium-Range Weather Forecasts (ECMWF) interim reanalysis (ERA-Interim) dataset (Dee et al., 2011; Žagar et al., 2011), with a horizontal resolution of 0.75°×0.75°. We used the monthly mean SST, precipitation and surface winds (i.e., winds at 10 meter) from 1979 to 2018. The SST and surface winds datasets of the ERA-Interim were downloaded from http://apps.ecmwf.int/datasets/data/interim-full-moda/levtype=sfc/. The precipitation data of ERA-Interim was provided by http://apps.ecmwf.int/datasets/data/interim-mdfa/levtype=sfc/. We also used the National Oceanic and Atmospheric Administration (NOAA) outgoing longwave radiation (OLR) dataset (Liebmann and Smith, 1996), with a horizontal resolution of 2.5°×2.5°. The OLR data was provided by https://psl.noaa.gov/data/gridded/data.olrcdr.interp.html. The climatology in this study was based on the period 1979-2018, and all data were detrended.

We defined the ITCZ using the monthly-mean precipitation exceeding 5 mm/day (Zhang, 2001; Gu et al., 2005; Yan and Li, 2018; Chen et al., 2021). The position of the ITCZ was identified by the latitude of the maximal zonal-mean rainfall (Adam et al., 2016a; Adam et al., 2016b; Yan and Li, 2018). The intensity of the ITCZ was evaluated by the amplitude of the zonal-mean rainfall.

To select the EP-type, CP-type and mixed-type El Niño events, we used the Niño-3 index (Kug et al., 2009) as the EP index, and the El Niño Modoki index (EMI) (Ashok et al., 2007) as the CP index. We calculated the EP indices and CP indices in January-February (JF) and March-April (MA) from 1979-2018 (Figure 1). If the EP indices (CP indices) in both JF and MA of a year exceed 0.95 standard deviations, this year is defined as the decaying year of an EP-type (CP-type) El Niño. The year that both EP indices and CP indices in JF and MA exceed approximately 0.8 standard deviation is defined as the decaying year of a mixed-type El Niño. According to this standard, there were five EP-type El Niños during 1979-2018, including the events of 1982/1983, 1986/1987, 1991/1992, 1997/1998 and 2015/2016; and five CP-type El Niños, including the events of 1990/1991, 1994/1995, 2002/2003, 2004/2005 and 2014/2015; and the 2009/2010 mixed-type El Niño.

To quantify the meridional SST structure, the meridional EP-type delta SST is defined as "$SSTA_{EQ} - 0.5 \times (SSTA_{SH} + SSTA_{NH})$" and CP-type delta SST is defined as "$SSTA_{NH} - SSTA_{SH}$". A positive EP-type delta SST indicates that the averaged equatorial SSTA was warmer than that within the northern and southern ITCZ regions. A positive CP-type delta SST indicates that the averaged SSTA within the northern ITCZ region is warmer than that within the

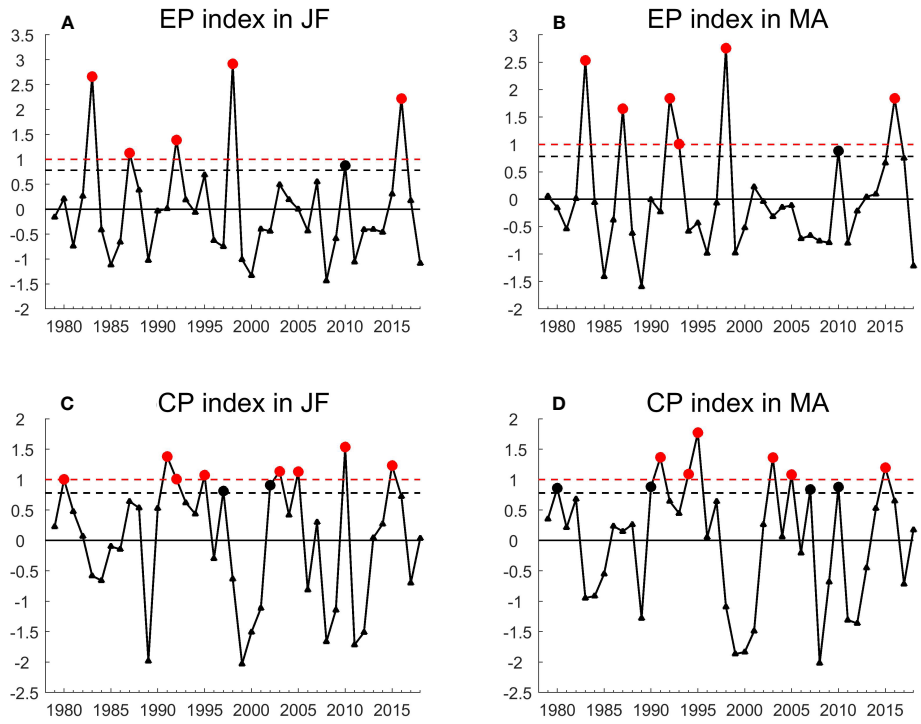

FIGURE 1
(A) EP index (i.e., Niño-3 index) and **(C)** CP index (i.e., EMI) in January-February; **(B)** EP index and **(D)** CP index in March-April from 1979 to 2018. Black (red) solid circles denote the decaying years of El Niño events with the index values exceeding 0.78 (1) standard deviation.

southern ITCZ region. To evaluate the latitude fluctuation and intensity asymmetry of double ITCZs, the change in distance between two ITCZs (Dis. Pre. Max) is identified as "anomalies for $|Lat_{precip.max.NH} - Lat_{precip.max.SH}|$", and precipitation difference between two ITCZs (delta Pre.) is identified as "$PA_{NH} - PA_{SH}$", respectively. We also defined the EP-type equatorial precipitation (EP-type EQ Pre.) as "$PA_{EQ} - 0.5 \times (PA_{SH} + PA_{NH})$" and CP-type equatorial precipitation (CP-type EQ Pre.) as "$PA_{EQ} - PA_{NH}$". These definitions of the relevant indices in this study are also listed in Table 1 for convenient viewing. Here, $SSTA_{EQ}$ (or $SSTA_{NH}$ or $SSTA_{SH}$) represents the averaged SSTA in the EQ (or NH, or SH) domain. PA_{EQ} (or PA_{NH}, or PA_{SH}) represents the averaged precipitation anomalies (PA) in the EQ (or NH, or SH) domain. EQ (or NH, or SH) region covers the area within (140°W–80°W, 1.5°S–1.5°N), or (140°W–80°W, 3.75°N–6.75°N), or (140°W–80°W, 3°S–6°S), respectively.

3 Results

3.1 Seasonal evolution

A seasonal evolution for climatic precipitation can be observed over the eastern Pacific Ocean (Figure 2A). For most time of a year, the ITCZ appears as an individual belt with heavy rainfall in the northern hemisphere (NH). In particular, an ITCZ also appears in the southern hemisphere (SH) in March-April. That is, double-ITCZ pattern emerges the eastern Pacific during boreal spring (Mitchell and Wallace, 1992; Zhang, 2001; Gu et al., 2005; Yan and Li, 2018; Chen et al., 2021). The two ITCZ bands are accompanied with strong convergence and the warmest SST.

For EP-type El Niños (Figure 2B), warm SSTs (larger than 27° C) at the equator persisted from January to May of the decaying year, replacing the climatic cold tongue. With the disappearance of the cold tongue during March-April, two ITCZs migrated to each other. Over the eastern Pacific Ocean, the climatic double-ITCZ pattern was replaced by an individual broad ITCZ band at the equator.

Unlike the EP-type El Niños, for CP-type El Niños (Figure 2C) the cold tongue further enhanced in March-April. With the strengthened cold tongue, the southern ITCZ disappeared. Consequently, the climatic double ITCZs changed to be an individual northern ITCZ band during the spring of the decaying year of CP-type El Niño.

For the 2009/2010 mixed-type El Niño (Figure 2D), during March-April of the decaying year, the cold tongue weakened. The two ITCZ bands with warm SSTs in NH and SH both moved equatorward. The convergence zone became wider and stronger covering the equator and the northern ITCZ, enhancing the northern ITCZ remarkably.

TABLE 1 The definitions of indices used in this study.

Index (Abbreviation)	Definition
EP-type delta SST	$SSTA_{EQ} - 0.5 \times (SSTA_{SH} + SSTA_{NH})$
CP-type delta SST	$SSTA_{NH} - SSTA_{SH}$
Dis. Pre. Max	Anomalies for $\lvert Lat_{precip.max.NH} - Lat_{precip.max.SH}\rvert$
delta Pre.	$PA_{NH} - PA_{SH}$
EP-type EQ Pre.	$PA_{EQ} - 0.5 \times (PA_{SH} + PA_{NH})$
CP-type EQ Pre.	$PA_{EQ} - PA_{NH}$

3.2 Meridional structure of SSTs and ITCZs in March-April

We analyzed the meridional structure of the zonal-mean precipitation in climatology and three types of El Niños in March-April of the decaying year (Figure 3A). For climatology, the maximum zonal-mean rainfall occurred on both sides of the equator, separated by a minimum equatorial rainfall. For EP-type El Niños, the southern ITCZ and northern ITCZ moved toward the equator, and the equatorial precipitation enhanced significantly, decreasing the north-south asymmetry. For CP-type El Niños, two ITCZs moved slightly northward, the northern ITCZ was further enhanced and the southern ITCZ almost disappeared, reinforcing the asymmetry of the double ITCZs. At the same time, the equatorial precipitation weakened.

For the 2009/2010 mixed-type El Niño (green in Figure 3A), both the southern and northern ITCZs moved equatorward, especially the southern ITCZ. Such migration led to a strengthened equatorial precipitation. This strengthened equatorial rainfall induced by mixed-type El Niño was smaller than that by the EP-type El Niño. Impacted by the mixed-type El Niño, the intensity of northern ITCZ increased, while the intensity of southern ITCZ decreased.

This work also investigates the meridional structures of anomalous SST and anomalous zonal-mean precipitation during March-April of the decaying years (Figures 3B–D).

For EP-type El Niños (Figure 3B), SST increased covering latitudes approximately from 20°S to 15°N. Although the warm SSTs emerged in a broad range, the maximum of SST warming occurred right over the equator. Considering that deep convections always situated on the warmest SST (e.g., Lindzen and Nigam, 1987; Zhang, 2001; Gu et al., 2005; Privé and Plumb, 2007; Schneider et al., 2014; Adam et al., 2016a; Adam et al., 2016b), the northern ITCZ and southern ITCZ migrated toward the equator, increasing the equatorial precipitation (more than 4mm/day).

For the CP-type El Niños (Figure 3C), anomalous zonal-mean SST pattern was asymmetric about the equator. The SST warming in the NH (Figure 3C) naturally contributed to a slight northward shift of both ITCZs (Figure 3A). This northward movement of ITCZs is consistent with the results of Kao and Yu (2009). Furthermore, the positive SST anomalies enhanced the intensity of the northern ITCZ; meanwhile the negative SST anomalies reduced the intensity of the southern ITCZ. Such changes of

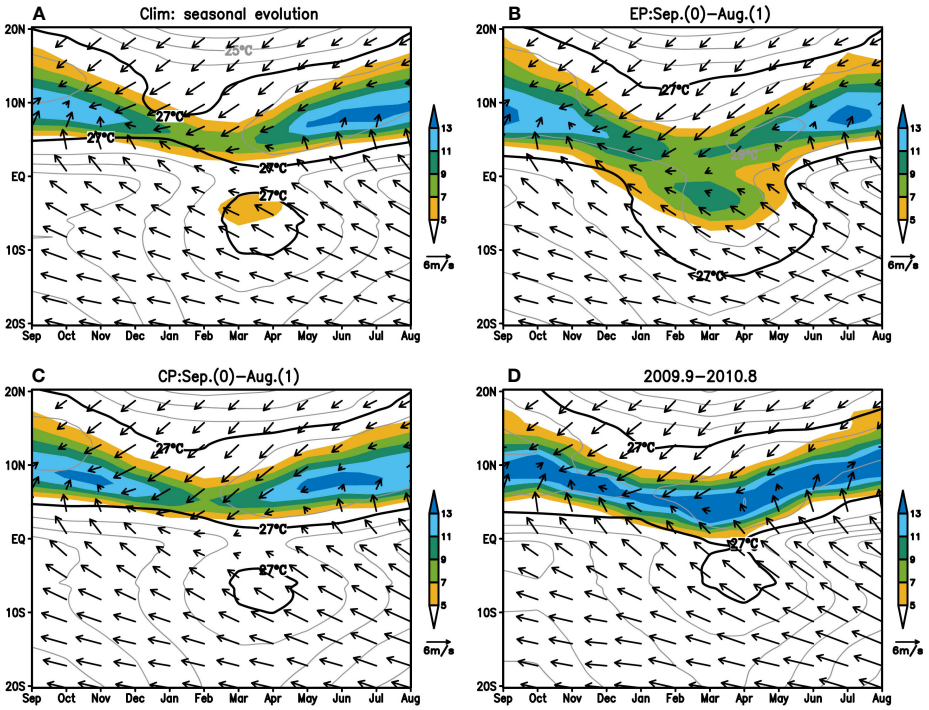

FIGURE 2
Seasonal evolution of zonal-mean rainfall (color shaded; units: mm/day), SST (contours; units: °C), and surface winds (vectors; units: m/s) over the eastern Pacific Ocean (140°W–80°W) for **(A)** the Climatology; **(B)** the composite of EP-type events; **(C)** the composite of CP-type events and **(D)** the 2009/2010 mixed-type event.

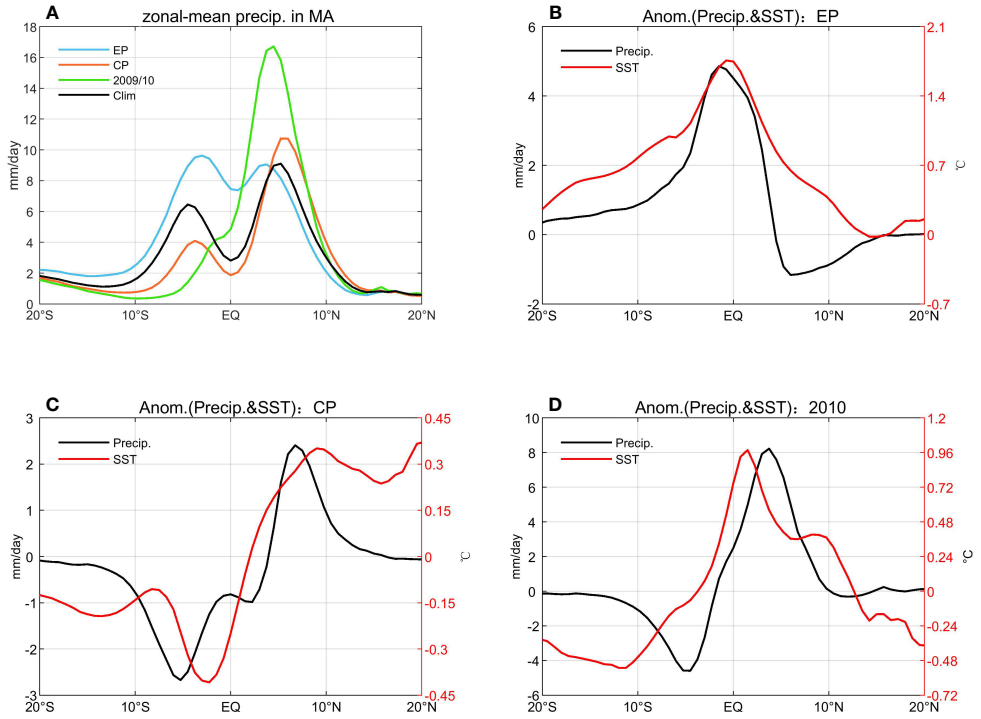

FIGURE 3
(A) zonal-mean precipitation (units: mm/day) over the eastern Pacific Ocean (140°W–80°W) in March-April for: composite of EP-type El Niños (blue), composite of CP-type El Niños (orange), 2009/2010 mixed-type El Niño (green) and climatology (black). Anomalous zonal-mean precipitation (black; units: mm/day) and SST (red; units: °C) for three types of El Niños in March-April: **(B)** the composite of EP-type El Niños; **(C)** the composite of CP-type El Niños and **(D)** the 2009/2010 mixed-type El Niño.

double ITCZs strengthened the north-south asymmetry of eastern Pacific. SST cooling at the equator weakened the equatorial precipitation. In addition, the latitude of the maximum (or minimum) of anomalous rainfall was not perfectly in consistent with the latitude of the maximum (or minimum) of anomalous SST. This is because the anomalous rainfall depends on not only the anomalous SST, but also the climatic SST and rainfall.

For the 2009/2010 mixed-type El Niño (Figure 3D), there was a meridional structure of SSTA with the warmest at the equator and relatively cold in the northern and southern sides of the equator. Influenced by a meridionally SST warming with a maximum at the equator (i.e., EP-type delta SST), the northern and southern ITCZs moved equatorward (especially the southern ITCZ), which led to an enhancement of equatorial precipitation. The weakened southern ITCZ moved equatorward, whereas the position of the strengthened northern ITCZ was basically unchanged. The equatorial precipitation increased by about 2 mm/day. Such enhancement of equatorial precipitation induced by the mixed-type El Niño was only half of that induced by EP-type El Niños.

At the same time, for this mixed-type El Niño (Figure 3D), a north-warm and south-cold contrast of SST anomalies (i.e., CP-type delta SST) caused a strengthened northern ITCZ and a weakened southern ITCZ. Precipitation in northern ITCZ increased by 8 mm/day, and that in southern ITCZ decreased by 4 mm/day. Therefore, compared with the climatologic asymmetry, the precipitation difference between two ITCZs further increased by 12 mm/day (Figure 3D). This enhancement of north-south asymmetry caused by mixed-type El Niño was twice that caused by CP-type El Niños.

In general, the regulation of the 2009/2010 event on double ITCZs not only reflects the modulation of EP-type El Niño, i.e., an increase of equatorial precipitation; but also the modulation of CP-type El Niño, i.e, the enhanced northern ITCZ and weakened southern ITCZ. Among them, the regulation characteristic of CP-type El Niño is more significant.

A previous study suggested that the strength of El Niño may affect the response of double ITCZs (e.g., Xie et al., 2018). We divided EP-type El Niños into extreme and moderate EP-type El Niños. It can be seen that the extreme (red solid lines in Figures 4A, C) and moderate (blue solid lines in Figures 4A, C) EP-type El Niños both exhibit the modulation features of the typical EP-type El Niño: the northern and southern ITCZs move equatorward, increasing the equatorial precipitation. The increase of equatorial precipitation is slightly stronger in extreme than in moderate EP-type El Niño events, which is due to higher SSTs and stronger deep convection in Niño-3 area in extreme events (Zheng et al., 2016; Xie et al., 2018). The intensities of CP-type El Niños are all moderate, and the five CP-type El Niños all exhibit the modulation features of the typical CP-type El Niño (Figures 4B, D). Basically, the regulation of an individual EP-type (CP-type) El Niño is in line with that of the typical EP-type (CP-type) El Niño.

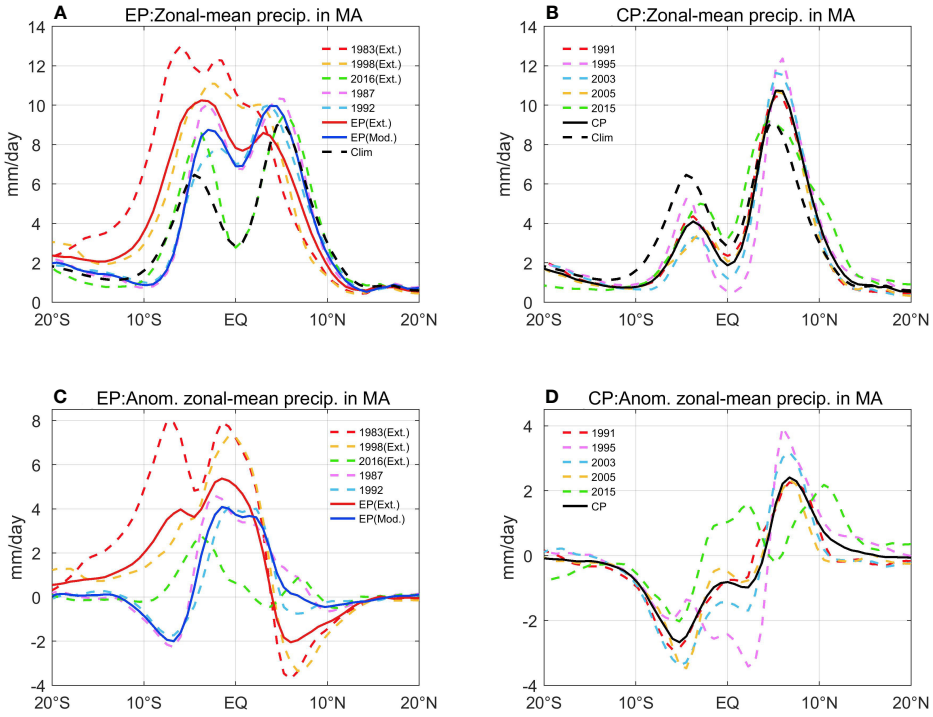

FIGURE 4
(A) zonal-mean precipitation (units: mm/day) over the eastern Pacific Ocean (140°W–80°W) in March-April for: composite of extreme EP-type El Niños (red solid line), composite of moderate EP-type El Niños (blue solid line), climatology (black dashed line) and individual EP-type El Niños (colored dashed lines). **(B)** zonal-mean precipitation over the eastern Pacific Ocean in March-April for: composite of CP-type El Niños (black solid line), climatology (black dashed line) and individual CP-type El Niños (colored dashed lines). **(C)** as in **(A)**, but for the anomalous zonal-mean precipitation. **(D)** as in **(B)**, but for the anomalous zonal-mean precipitation.

3.3 Spatial distributions in March-April

For climatology (Figure 5A), a distinctive double-ITCZ pattern appeared over the eastern Pacific Ocean in March-April. Two zonally elongated intense precipitation bands were situated straddling the equator. These two ITCZs are confined to the domain where SST was larger than 27°C. In addition, northeasterlies and cross-equatorial southeasterlies converged in the northern ITCZ.

We also analyzed the spatial distribution of anomalies over the eastern Pacific Ocean in March-April of the decaying year of three types of El Niños, respectively (Figures 5B–D).

During the spring of the following year of EP-type events (Figure 5B), zonally the SST warming larger than 1°C covered the entire tropical eastern Pacific Ocean, and the SST warming could reached more than 2.5°C off the West Coast of South America. Meridionally, the strongest SST warming and the anomalous convergence occurred at the equator (3°S–3°N) (Figure 5B). Two ITCZs both moved equatorward, resulting in significantly enhanced equatorial precipitation across the tropical eastern Pacific Ocean.

During the spring of the following year of CP-type events (Figure 5C), there was a weak SST cooling over the tropical eastern Pacific, and a SST cooling above 0.5°C off the West Coast of South America. Meridionally, the positive SSTs occurred north of the equator; while the negative SSTs occurred south the equator, with the strongest cooling approximately at 2°S. Accompanying the SST warmings in the NH, a convergence of anomalous winds appeared at around 6°N. Naturally, this north-warm and south-cold SSTA structure linked to a strengthened northern ITCZ and a weakened southern ITCZ.

During the spring of 2010 (Figure 5D), zonally SST warming larger than 0.5°C covered the entire tropical eastern Pacific Ocean. A wide range of SST cooling emerged south of 2°S and east of 130° W to the west coast of South America. The meridionally SST warming occurred at the equator and north of the equator, with the maximum warming occurring at the equator. Cross- equatorial southerlies strengthened. Convergence at the equator and in the northern ITCZ enhanced, while convergence in the southern ITCZ weakened. Hence, precipitation at the equator and in the northern ITCZ strengthened and precipitation in the southern ITCZ was suppressed.

ITCZ precipitation is highly linked with the cloud cover over the tropics. Low-value OLR or negative anomalous OLR represents deep convective cloud. We also examined the OLR spatial distribution in March-April (Figure 6). For climatology (Figure 6A), besides the active convection within northern ITCZ region, a zonally elongated active convection band also emerges within the southern ITCZ region. For EP-type El Niños (Figure 6B), accompanying the equatorial westerlies, anomalous convergences occurred at the equator and deep convective clouds covered the entire tropical eastern Pacific Ocean. For CP-type El Niños (Figure 6C), accompanying the cross-equatorial southeasterlies,

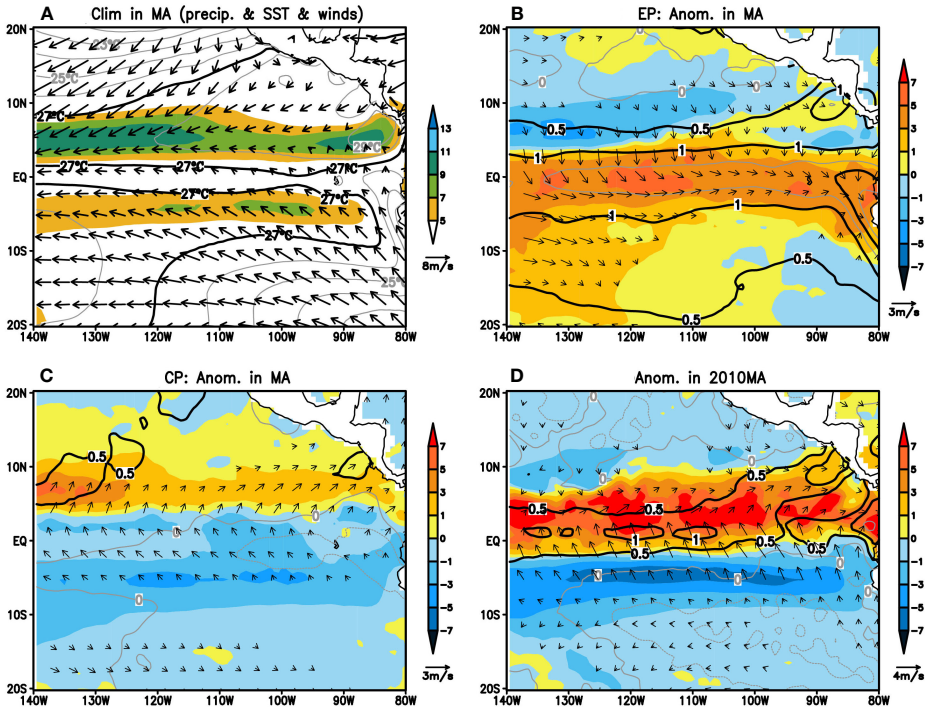

FIGURE 5
(A) Climatology in March-April: spatial pattern of the precipitation (color shaded; units: mm/day), SST (contours; units: °C), and surface winds (vectors; units: m/s; wind speed smaller than 1 m/s has been masked out) over the tropical eastern Pacific Ocean. Anomalies of precipitation, SST and surface winds (wind speed smaller than 0.5 m/s has been masked out) for: **(B)** the composite of EP-type El Niños; **(C)** the composite of CP-type El Niños and **(D)** the 2009/2010 mixed-type El Niño.

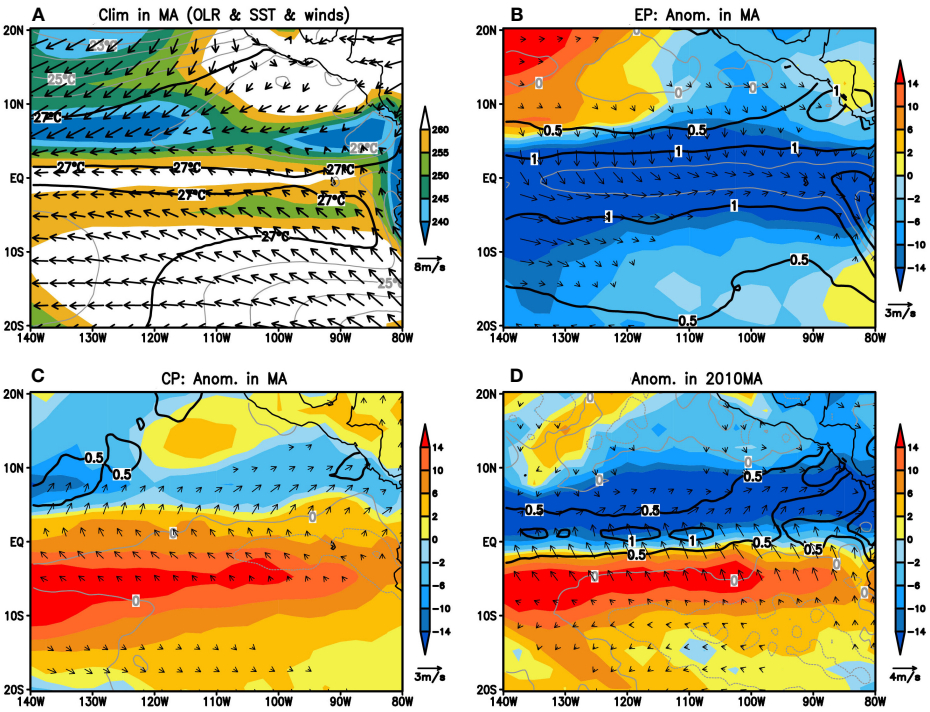

FIGURE 6
As in Figure 5, but color shaded for the outgoing longwave radiation (OLR, units: W/m^2).

anomalous convergence occurred north of the equator and deep convective cloud covered the tropical eastern Pacific Ocean north of 5°N. For the 2009/2010 mixed-type El Niño (Figure 6D), accompanying the cross-equatorial southeasterlies, anomalous convergence occurred at the equator and north of the equator. Deep convective clouds covered the equatorial region and northern ITCZ region for this mixed-type El Niño.

3.4 Modulation of meridional EP-type and CP-type delta SST on double ITCZs

3.4.1 Relationship between SST and double ITCZs in March-April for 2009/2010 mixed-type El Niño

As described in Section 3.2, the SST meridional structure is closely linked to the position and intensity of double ITCZs. For the 2009/2010 event, EP index and EP-type delta SST were both positive, indicating that when the SST in the equatorial eastern Pacific was warming, the meridional SSTA was the warmest at the equator (green star in Figure 7A). For the 2009/2010 event, the CP index and CP-type delta SST were both positive, too. This suggested that when there was a "negative-positive-negative" SSTA zonal distribution in the equatorial Pacific, a north-warm and south-cold SSTA meridional structure occurred over the eastern Pacific at the same time (green star in Figure 7D). In other words, for the 2009/2010 mixed-type El Niño, meridional EP-type delta SST pattern and CP-type delta SST pattern co-emerged.

EP-type delta SST mainly modulates the position of the double ITCZs (Figure 7B), while CP-type delta SST mainly modulates the intensity of the double ITCZs (Figure 7E). In the 2009/2010 event, the EP-type delta SST was positive, and the corresponding change of meridional distance between two ITCZs was negative (green star in Figure 7B). This indicated that the meridional SSTA structure with the maximum warming at the equator drove the two ITCZs to migrate toward each other, reducing the distance between them. In the 2009/2010 mixed-type El Niño, the regulation of EP-type delta SST on the position of double ITCZs worked (green star in Figure 7B). In addition, accompanying the positive CP-type delta SST, the delta precipitation between two ITCZs (green star in Figure 7E) was large and positive. This suggested that the "north-warm and south-cold" meridional SSTA structure would lead to a stronger precipitation north of the equator, and a weaker precipitation south of the equator, increasing the north-south asymmetry of double ITCZs. In the 2009/2010 mixed-type El Niño, the regulation of CP-type delta SST on the intensity of double ITCZs also worked (green star in Figure 7E).

In the 2009/2010 event, regulated by EP-type delta SST, a warmer SSTA at the equator drove the northern and southern ITCZs to shift toward the equator, resulting in an increasing equatorial precipitation over the eastern Pacific Ocean (green star in Figure 7C). Regulation of

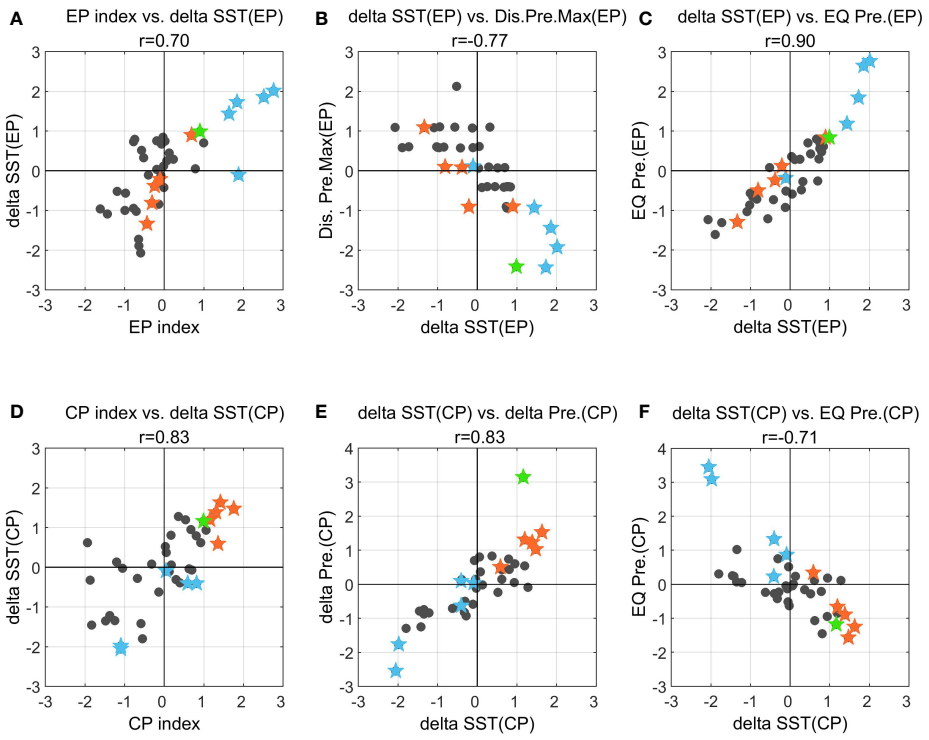

FIGURE 7
(A) EP index versus EP-type delta SST; **(B)** EP-type delta SST versus change in distance between two ITCZs; **(C)** EP-type delta SST versus EP-type equatorial precipitation; **(D)** CP index versus CP-type delta SST; **(E)** CP-type delta SST versus delta precipitation; **(F)** CP-type delta SST versus CP-type equatorial precipitation. For each subfigure, solid stars denote the El Niño decaying years: EP-type (blue), CP-type (orange) and the 2009/2010 mixed-type (green). All these indices are calculated for March-April and are normalized. In all subfigures, the correlations pass confidence test at a 99% confidence level.

the CP-type delta SST on double ITCZs is as follows. The "north-warm and south-cold" meridional structure of SSTA strengthened the precipitation north of the equator and weakened the precipitation south of the equator. In addition, compared with the increase in equatorial precipitation, the precipitation in northern ITCZ increased more (green star in Figure 7F).

3.4.2 The evolution of EP-type delta SST and CP-type delta SST over the eastern Pacific Ocean

Figures 8 shows the evolution of EP-type delta SST for three different types of El Niños. For EP-type El Niños (Figure 8A), in March-April of the decaying year, the EP-type delta SST was positive over the entire eastern Pacific Ocean with an intensity approximately from 0.5 to 1°C. Whereas for CP-type El Niños (Figure 8B), in March-April of the decaying year, the EP-type delta SST was basically negative over the entire eastern Pacific Ocean. For the 2009/2010 mixed El Niño (Figure 8C), a positive EP-type delta SST emerged over the entire eastern Pacific in March-April of 2010. Like typical EP-type El Niños, during the spring of the decaying year of mixed-type El Niño (Figure 8C), SST anomalies were the warmest at the equator (represented by positive EP-type delta SST), which was favorable to an enhancement of equatorial precipitation.

Figure 9 demonstrates the evolution of CP-type delta SST for three different types of El Niños. During March-April of the EP-type El Niños' decaying year (Figure 9A), a negative CP-type delta SST covered the eastern Pacific, indicating a north-cold and south-warm SSTA structure. While during March-April of the CP-type El Niños' decaying year (Figure 9B), a positive CP-type delta SST covered the eastern Pacific, indicating a north-warm and south-cold SSTA structure. Like typical CP-type El Niños, during the spring of the decaying year of mixed-type El Niño, a north-warm and south-cold SSTA pattern appeared over the eastern Pacific (represented by positive CP-type delta SST) (Figure 9C), which favored a strengthening northern ITCZ and a weakening southern ITCZ.

3.4.3 Possible explanations for a weakened (an amplified) regulation of EP-type (CP-type) delta SST

In March-April period of EP-type El Niños' decaying year, the values of EP index were large and positive, exceeding 1°C; the values of CP index were close to zero (Figure 10A). For these typical EP-type El Niños, the values of EP-type delta SST were positive and CP-type delta SST were negative and weak (Figure 10B), implying a typical regulation of meridional EP-type delta SST structure.

In contrast, in March-April period of CP-type El Niños' decaying year, the values of CP index were large and positive, approximately 0.8°C; the values of EP index were close to zero (Figure 10C). For these typical CP-type El Niños, the values of CP-type delta SST were positive and EP-type delta SST were negative and weak (Figure 10D), implying a typical regulation of meridional CP-type delta SST structure.

The 2009/2010 mixed-type El Niño has the characteristics of both EP-type and CP-type El Niños. In March-April of 2010, the values of EP index and CP index were both positive (Figure 10E). Accordingly, the EP-type delta SST and CP-type delta SST were both positive (about 0.5°C) (Figure 10F), indicating that the EP-type delta SST and CP-type delta SST co-worked for a mixed-type El Niño.

Although the amplitudes of the two types of delta SST were comparable (both about 0.5°C), the modulation of mixed-type El

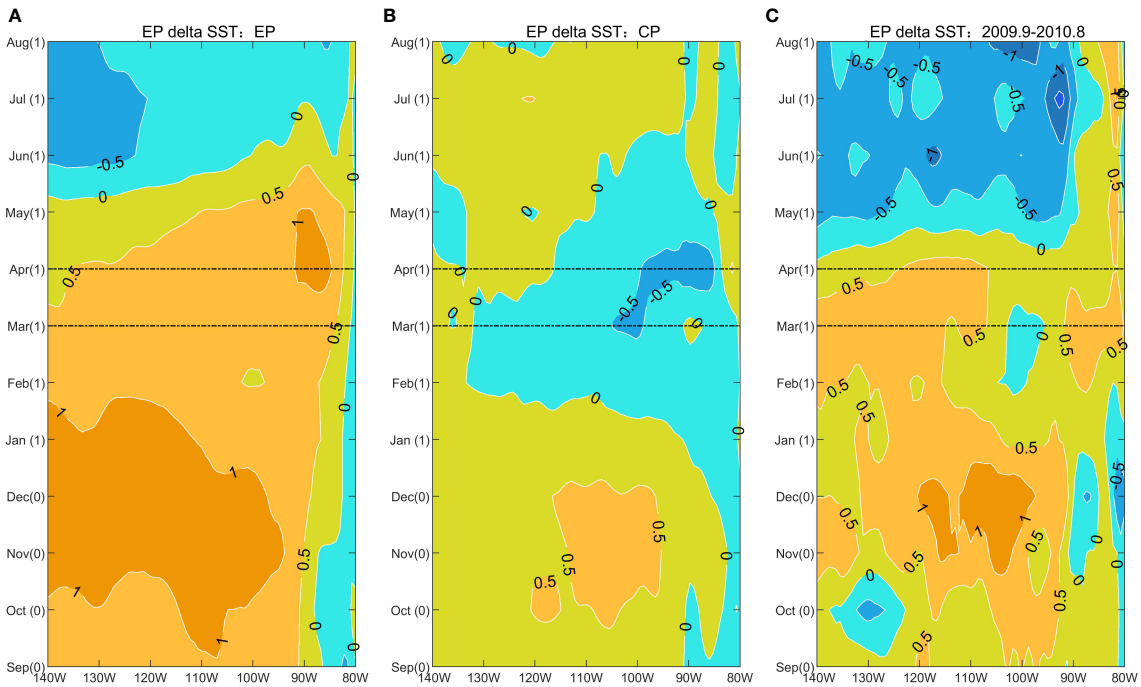

FIGURE 8
Time evolution of the EP-type delta SST over the eastern Pacific Ocean (140°W–80°W) during three types of El Niño years: **(A)** the composite of EP-type El Niños; **(B)** the composite of CP-type El Niños and **(C)** the 2009/2010 mixed-type El Niño. The numbers in parentheses following the months are 0 for the developing year and 1 for the decaying year of El Niño.

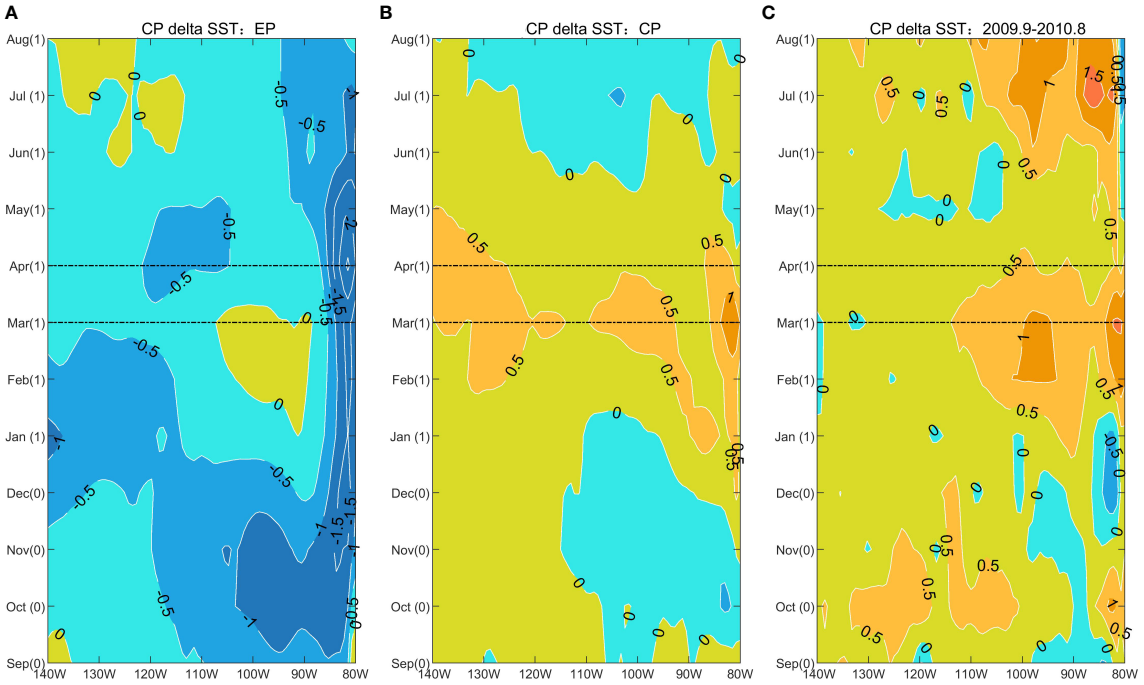

FIGURE 9
As in Figure 8, but for time evolution of the CP-type delta SST.

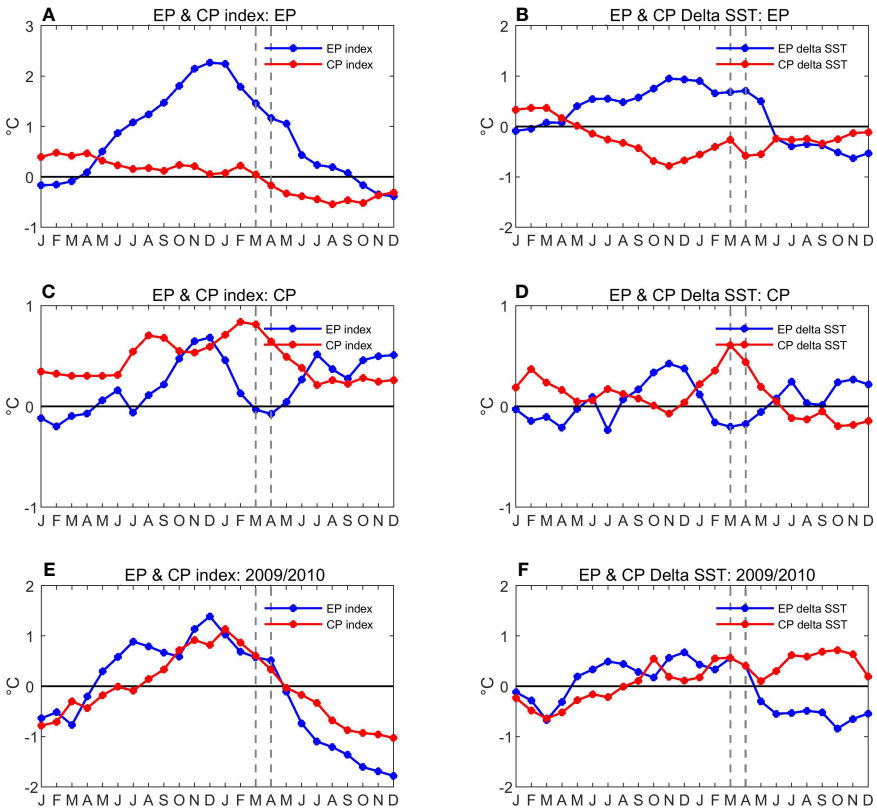

FIGURE 10
Time evolution of EP and CP index (subfigures of left column) for: **(A)** the composite of EP-type El Niños; **(C)** the composite of CP-type El Niños and **(E)** the 2009/2010 mixed-type El Niño. Time evolution of zonal-mean EP-type and CP-type delta SST (subfigures of right column) for: **(B)** the composite of EP-type El Niños; **(D)** the composite of CP-type El Niños and **(F)** the 2009/2010 mixed-type El Niño.

Niño on double ITCZs was eventually similar to that of CP-type El Niños. The possible explanations are analyzed as follows.

The EP-type delta SST itself for mixed-type event (blue in Figure 10F) was weaker than that of typical EP-type events (blue in Figure 10B). The maximum SST anomaly of mixed-type event was located at 2°N (Figure 3D), unlike typical EP-type event, which are located exactly at the equator (Figure 3B). Regulated by the positive EP-type delta SST in mixed-type El Niño, southern and northern ITCZs moved toward equator. Among them, the southern ITCZ moved greatly towards equator, while the northern ITCZ moved very slightly towards the equator. At the same time, regulated by the positive CP-type delta SST in mixed-type El Niño, southern ITCZ was weakened and northern ITCZ was strengthened. Overall, the weakened southern ITCZ migrating equatorward could not provide much rainfall for the equatorial region; while the strengthened northern ITCZ almost stayed in its climatic position. Thus, the increase of equatorial precipitation in mixed-type El Niño was much smaller than that in typical EP-type El Niños.

The CP-type delta SST for mixed-type event (red in Figure 10F) was comparable to that of typical CP-type events (red in Figure 10D). In fact, CP-type delta SST in mixed-type event can be mainly attributed to the warm SST anomalies within the northern ITCZ region (Figure 3D); while CP-type delta SST in CP-type event is jointly induced by both the warm SST anomalies within the northern ITCZ region and the cold SST anomalies within the southern ITCZ region (Figure 3C). Taking the northern ITCZ into account, the positive SST anomaly in the mixed-type event was twice that in typical CP-type events. Therefore, the precipitation increase in the northern ITCZ in the mixed-type event was much stronger than that in the typical CP-type event. The meridional SST structure of the mixed-type El Niño was manifested as an "equator-warmest, north-warm and south-cold" structure, driving the southern ITCZ branch shift toward the equator and the northern hemisphere. Such northward movement of southern ITCZ in the mixed-type El Niño was more significant than that in the typical EP-type El Niños, and the precipitation within the region of climatic southern ITCZ was significantly reduced. Therefore, the enhancement of north-south asymmetry of double ITCZs in mixed-type El Niño was much larger than that in CP-type El Niños.

4 Discussion and conclusions

A north-dominant and south-secondary double-ITCZ pattern emerges over the eastern Pacific Ocean in March-April. This study examines the regulation of the 2009/2010 mixed-type El Niño on the double ITCZs during the spring of El Niño's decaying year. This study also contrasts the modulations of the mixed-type El Niño with those of the typical EP-type and CP-type El Niños.

Our results show that in March-April of the mixed-type El Niño decaying year 2010, a meridionally "equator-warmest, north-warm and south-cold" SSTA structure emerged over the eastern Pacific Ocean. This meridional SSTA pattern was a combination of "SST warming with a maximum at the equator" (i.e., EP-type delta SST) and "north-warm and south-cold" (i.e., CP-type delta SST) patterns.

In the mixed-type El Niño, both EP-type and CP-type delta SST played a role and had corresponding climate impacts. We analyzed the climate effects from two perspectives: the equatorial precipitation and the north-south asymmetry of double ITCZs. (1) Regarding the equatorial precipitation: Regulated by EP-type delta SST, southern ITCZ and northern ITCZ moved equatorward, especially the southern ITCZ. At the same time, regulated by CP-type delta SST, southern (northern) ITCZ was weakened (enhanced). The weakened southern ITCZ could not provide much rainfall for the equatorial region; the enhanced northern ITCZ only moved slightly towards the equator. Therefore, the increase of equatorial precipitation in the mixed-type El Niño (approximately 2 mm/day) was only half of that in the typical EP-type El Niños. (2) Regarding north-south asymmetry of double ITCZs: Regulated by CP-type delta SST, the northern ITCZ was significantly enhanced and the southern ITCZ was weakened. At the same time, regulated by EP-type delta SST, southern ITCZ branch shifted equatorward, inducing a further precipitation decrease within the climatic southern ITCZ region. Therefore, the north-south asymmetry of double ITCZs in the mixed-type El Niño (approximately 12 mm/day) was more than twice that in the typical CP-type El Niños.

Under the coordinated modulation of EP-type and CP-type delta SST in a mixed-type El Niño, the climate effect of EP-type delta SST (increasing equatorial precipitation) is weakened; while the climate effect of CP-type delta SST (enhancing the northern ITCZ and weakening the southern ITCZ) is amplified. The climate effect of mixed-type El Niño finally resembles that of typical CP-type El Niños, intensifying the north-south asymmetry of the eastern Pacific double ITCZs.

The double ITCZs and El Niño interact with each other in observation and model experiments (e.g., Xie et al., 2018; Peng et al., 2020). The impact of ITCZs on El Niño depends on whether the westerly wind anomaly or the cross-equatorial southeasterly wind anomaly dominates in the eastern Pacific. Previous studies (Xie et al., 2018; Peng et al., 2020) suggested that during boreal spring westerly wind anomalies caused by deep convections suppressed the ocean upwelling in the eastern Pacific, which was favorable to the maintenance of El Niños; while the cross-equatorial southeasterly wind anomalies enhanced the ocean upwelling south of the equator, inducing a rapid decay of El Niños. During the spring of 2010 (Figures 5D and 6D), the SST warming emerged in both the equatorial and northern ITCZ regions. The equatorial precipitation and northern ITCZ both strengthened, especially the northern ITCZ. Accompanying the strongest deep convection in the northern ITCZ region (Figure 6D), C-shaped wind anomalies that converged towards the northern ITCZ emerged over the eastern Pacific Ocean. The cross-equatorial southeasterly wind anomalies dominated at the equator (Figures 5D and 6D). These cross-equatorial southeasterly wind anomalies strengthened the ocean upwelling south of the equator, promoting a rapid decay of the mixed-type El Niño event.

The double-ITCZ bias widely exists in climate models (e.g., Li and Xie, 2014; Adam et al., 2018; Tian and Dong, 2020; Samuels et al., 2021) and boreal spring is the season that provides the largest contribution to the annual-mean double-ITCZ bias (e.g., Si et al., 2021). In the Coupled Model Intercomparison Project Phase 5

(CMIP5), CP-type El Niños are under-represented (e.g., Adam et al., 2018). Compared with CMIP3 (Meehl et al., 2007) or CMIP5 (Taylor et al., 2012), there are some improvements in reducing the double-ITCZ bias in CMIP6 (e.g., Eyring et al., 2016; Tian and Dong, 2020; Si et al., 2021; Ma et al., 2023). Increased resolution in CMIP6 is able to reduce the positive precipitation bias over the tropical southern Atlantic Ocean, but it could not reduce the double-ITCZ bias over the Pacific Ocean (Ma et al., 2023). Reducing the double-ITCZ bias over the Pacific Ocean in the climate model remains a challenge (e.g., Fiedler et al., 2020; Tian and Dong, 2020; Samuels et al., 2021). ENSO diversity has increased in recent decades (e.g., Capotondi et al., 2015; Santoso et al., 2017). For instance, CP-type El Niños have increased since 2000, and 2009/2010 mixed-type El Niño has also occurred. This study will contribute to a better understanding of the impacts of ENSO diversity on double ITCZs in the eastern Pacific region. This also provides a new perspective to improve the simulation of ITCZs over the Pacific Ocean in climate models.

Data availability statement

The original contributions presented in the study are included in the article/supplementary material. Further inquiries can be directed to the corresponding authors.

Author contributions

LY and JX initiated the idea, designed the study. YC and LY analyzed the data and contributed to the writing of the manuscript. JX, SZ, GC and PL revised and edited the manuscript. All authors contributed to the article and approved the submitted version.

Funding

This study was jointly supported by the National Natural Science Foundation of China (42130605), Shenzhen Science and Technology Program (JCYJ20210324131810029), the Strategic Priority Research Program of Chinese Academy of Sciences (XDA20060503), the National Key R&D Program of China (Grant 2018YFC1505902) and program for scientific research start-up funds of Guangdong Ocean University (R19061 & R18023).

Conflict of interest

The authors declare that the research was conducted in the absence of any commercial or financial relationships that could be construed as a potential conflict of interest.

Publisher's note

All claims expressed in this article are solely those of the authors and do not necessarily represent those of their affiliated organizations, or those of the publisher, the editors and the reviewers. Any product that may be evaluated in this article, or claim that may be made by its manufacturer, is not guaranteed or endorsed by the publisher.

References

Adam, O., Bischoff, T., and Schneider, T. (2016a). Seasonal and interannual variations of the energy flux equator and ITCZ. part I: Zonally averaged ITCZ position. *J. Clim.* 29, 3219–3230. doi: 10.1175/JCLI-D-15-0512.1

Adam, O., Bischoff, T., and Schneider, T. (2016b). Seasonal and interannual variations of the energy flux equator and ITCZ. part II: Zonally varying shifts of the ITCZ. *J. Clim.* 29, 7281–7293. doi: 10.1175/JCLI-D-15-0710.1

Adam, O., Schneider, T., and Brient, F. (2018). Regional and seasonal variations of the double-ITCZ bias in CMIP5 models. *Clim. Dyn.* 51 (1–2), 101–117. doi: 10.1007/s00382-017-3909-1

Ashok, K., Behera, S. K., Rao, S. A., Weng, H., and Yamagata, T. (2007). El Niño modoki and its possible teleconnection. *J. Geophys. Res. Oceans* 112, C11007. doi: 10.1029/2006JC003798

Cao, X., Chen, G., and Chen, W. (2013). Tropical cyclogenesis induced by ITCZ breakdown in association with synoptic wave train over the western north pacific. *Atmos. Sci. Lett.* 14 (4), 294–300. doi: 10.1002/asl2.452

Capotondi, A., Wittenberg, A. T., Newman, M., Di Lorenzo, E., Yu, J. Y., Braconnot, P., et al. (2015). Understanding ENSO diversity. *Bull. Am. Meteorol. Soc* 96, 921–938. doi: 10.1175/BAMS-D-13-00117.1

Chen, Y., Yan, L., Li, G., Xu, J., Long, J., and Zheng, S. (2021). Contrasting impacts of three extreme El niños on double ITCZs over the Eastern pacific ocean. *Atmos.* 12, 424. doi: 10.3390/atmos12040424

Dee, D. P., Uppala, S. M., Simmons, A., Berrisford, P., Poli, P., Kobayashi, S., et al. (2011). The ERA-interim reanalysis: Configuration and performance of the data assimilation system. *Q. J. R. Meteor. Soc* 137, 553–597. doi: 10.1002/qj.828

Eyring, V., Bony, S., Meehl, G. A., Senior, C. A., Stevens, B., Stouffer, R. J., et al. (2016). Overview of the coupled model intercomparison project phase 6 (CMIP6) experimental design and organization. *Geoscientific Model. Dev.* 9 (5), 1937–1958. doi: 10.5194/gmd-9-1937-2016

Fiedler, S., Crueger, T., D'Agostino, R., Peters, K., Becker, T., Leutwyler, D., et al. (2020). Simulated tropical precipitation assessed across three major phases of the coupled model intercomparison project (CMIP). *Mon. Weather Rev.* 148 (9), 3653–3680. doi: 10.1175/MWR-D-19-0404.1

Gu, G., Adler, R. F., and Sobel, A. H. (2005). The eastern pacific ITCZ during the boreal spring. *J. Atmos. Sci.* 62, 1157–1174. doi: 10.1175/JAS3402.1

Haffke, C., Magnusdottir, G., Henke, D., Smyth, P., and Peings, Y. (2016). Daily states of the march–April East pacific ITCZ in three decades of high-resolution satellite data. *J. Clim* 29 (8), 2981–2995. doi: 10.1175/JCLI-D-15-0224.1

Henke, D., Smyth, P., Haffke, C., and Magnusdottir, G. (2012). Automated analysis of the temporal behavior of the double intertropical convergence zone over the east pacific. *Remote Sens. Environ.* 123, 418–433. doi: 10.1016/j.rse.2012.03.022

Kao, H. Y., and Yu, J. Y. (2009). Contrasting eastern-pacific and central-pacific types of ENSO. *J. Clim.* 22, 615–632. doi: 10.1175/2008JCLI2309.1

Kim, W. M., Yeh, S. W., Kim, J. H., and Kug, J. S. (2011). The unique 2009–2010 El niño event: A fast phase transition of warm pool El niño to la niña. *Geophys. Res. Lett.* 38 (15), L15809. doi: 10.1029/2011GL048521

Kug, J. S., Jin, F. F., and An, S. I. (2009). Two types of El niño events: cold tongue El niño and warm pool El niño. *J. Clim.* 22, 1499–1515. doi: 10.1175/2008JCLI2624.1

Larkin, N. K., and Harrison, D. (2005). On the definition of El niño and associated seasonal average US weather anomalies. *Geophys. Res. Lett.* 32, L13705. doi: 10.1029/2005GL022738

Li, G., Ren, B., Yang, C., and Zheng, J. (2010). Indices of El niño and El niño modoki: an improved El niño modoki index. *Adv. Atmos. Sci.* 27, 1210–1220. doi: 10.1007/s00376-010-9173-5

Li, G., and Xie, S. P. (2014). Tropical biases in CMIP5 multimodel ensemble: The excessive equatorial pacific cold tongue and double ITCZ problems. *J. Clim.* 27 (4), 1765–1780. doi: 10.1175/JCLI-D-13-00337.1

Liebmann, B., and Smith, C. A. (1996). Description of a complete (interpolated) outgoing longwave radiation dataset. *Bull. Amer. Meteor. Soc.* 77, 1275–1277. Available at: https://www.jstor.org/stable/26233278

Lietzke, C. E., Deser, C., and Vonder Haar, T. H. (2001). Evolutionary structure of the eastern pacific double ITCZ based on satellite moisture profile retrievals. *J. Clim.* 14, 743–751. doi: 10.1175/1520-0442(2001)014<0743:ESOTEP>2.0.CO;2

Lindzen, R. S., and Nigam, S. (1987). On the role of sea surface temperature gradients in forcing low-level winds and convergence in the tropics. *J. Atmos. Sci.* 44, 2418–2436. doi: 10.1175/1520-0469(1987)044<2418:OTROSS>2.0.CO;2

Ma, X., Zhao, S., Zhang, H., and Wang, W. (2023). The double-ITCZ problem in CMIP6 and the influences of deep convection and model resolution. *Int. J. Climatol.* 43, 1–22. doi: 10.1002/joc.7980

Meehl, G. A., Covey, C., Delworth, T., Latif, M., McAvaney, B., Mitchell, J. F., et al. (2007). The WCRP CMIP3 multimodel dataset: A new era in climate change research. *Bull. Am. Meteorol. Soc* 88 (9), 1383–1394. doi: 10.1175/BAMS-88-9-1383

Mitchell, T. P., and Wallace, J. M. (1992). The annual cycle in equatorial convection and sea surface temperature. *J. Clim.* 5, 1140–1156. doi: 10.1175/1520-0442(1992)005<1140:TACIEC>2.0.CO;2

Peng, Q., Xie, S.-P., Wang, D., Kamae, Y., Zhang, H., Hu, S., et al. (2020). Eastern Pacific wind effect on the evolution of El niño: implications for ENSO diversity. *J. Clim.* 33, 3197–3212. doi: 10.1175/JCLI-D-19-0435.1

Philander, S., Gu, D., Lambert, G., Li, T., Halpern, D., Lau, N., et al. (1996). Why the ITCZ is mostly north of the equator. *J. Clim.* 9, 2958–2972. doi: 10.1175/1520-0442(1996)009<2958:WTIIMN>2.0.CO;2

Privé, N. C., and Plumb, R. A. (2007). Monsoon dynamics with interactive forcing. part I: Axisymmetric studies. *J. Atmos. Sci.* 64, 1417–1430. doi: 10.1175/JAS3916.1

Rasmusson, E. M., and Carpenter, T. H. (1982). Variations in tropical sea surface temperature and surface wind fields associated with the southern Oscillation/El niño. *Mon. Weather Rev.* 110, 354–384. doi: 10.1175/1520-0493(1982)110<0354:VITSST>2.0.CO;2

Samuels, M., Adam, O., and Gildor, H. (2021). A shallow thermocline bias in the southern tropical pacific in CMIP5/6 models linked to double-ITCZ bias. *Geophys. Res. Lett.* 48, e2021GL093818. doi: 10.1029/2021GL093818

Santoso, A., Mcphaden, M. J., and Cai, W. (2017). The defining characteristics of ENSO extremes and the strong 2015/2016 El niño. *Rev. Geophys.* 55, 1079–1129. doi: 10.1002/2017RG000560

Schneider, T., Bischoff, T., and Haug, G. H. (2014). Migrations and dynamics of the intertropical convergence zone. *Nature* 513, 45–53. doi: 10.1038/nature13636

Si, W., Liu, H., Zhang, X., and Zhang, M. (2021). Double intertropical convergence zones in coupled ocean-atmosphere models: Progress in CMIP6. *Geophys. Res. Lett.* 48, e2021GL094779. doi: 10.1029/2021GL094779

Taylor, K. E., Stouffer, R. J., and Meehl, G. A. (2012). An overview of CMIP5 and the experiment design. *Bull. Am. Meteorol. Soc* 93 (4), 485–498. doi: 10.1175/BAMS-D-11-00094.1

Tian, B., and Dong, X. (2020). The double-ITCZ bias in CMIP3, CMIP5 and CMIP6 models based on annual mean precipitation. *Geophys. Res. Lett.* 47, e2020GL087232. doi: 10.1029/2020GL087232

Xie, S. P., Peng, Q., Kamae, Y., Zheng, X. T., Tokinaga, H., and Wang, D. (2018). Eastern Pacific ITCZ dipole and ENSO diversity. *J. Clim.* 31, 4449–4462. doi: 10.1175/JCLI-D-17-0905.1

Xie, R., and Yang, Y. (2014). Revisiting the latitude fluctuations of the eastern pacific ITCZ during the central pacific El niño. *Geophys. Res. Lett.* 41, 7770–7776. doi: 10.1002/2014GL061857

Yan, L., and Li, G. (2018). Double intertropical convergence zones over the eastern pacific ocean: Contrasting impacts of the eastern pacific-and central pacific-type El niños. *Atmos. Sci. Lett.* 19, e852. doi: 10.1002/asl.852

Yu, J. Y., and Kim, S. T. (2013). Identifying the types of major El niño events since 1870. *Int. J. Climatol.* 33, 2105–2112. doi: 10.1002/joc.3575

Žagar, N., Skok, G., and Tribbia, J. (2011). Climatology of the ITCZ derived from ERA interim reanalyses. *J. Geophys. Res. Atmos.* 116, D15103. doi: 10.1029/2011JD015695

Zhang, C. (2001). Double ITCZs. *J. Geophys. Res. Atmos.* 106, 11785–11792. doi: 10.1029/2001JD900046

Zhang, W., Jin, F. F., Zhao, J. X., Qi, L., and Ren, H. L. (2013). The possible influence of a nonconventional El niño on the severe autumn drought of 2009 in southwest China. *J. Clim.* 26 (21), 8392–8405. doi: 10.1175/JCLI-D-12-00851.1

Zheng, X. T., Xie, S.-P., Lv, L. H., and Zhou, Z. Q. (2016). Intermodel uncertainty in ENSO amplitude change tied to pacific ocean warming pattern. *J. Clim.* 29, 7265–7279. doi: 10.1175/JCLI-D-16-0039.1

Zhu, J., Liu, Y., Xie, R., and Chang, H. (2018). A comparative analysis of the impacts of two types of El niño on the central and Eastern pacific ITCZ. *Atmos.* 9, 266. doi: 10.3390/atmos9070266